Available online at www.sciencedirect.com
SCIENCE DIRECT®
International Journal of Heat and Mass Transfer 48 (2005) 3506–3515
International Journal of HEAT and MASS TRANSFER
www.elsevier.com/locate/ijhmt

Estimation of the periodic thermal conditions on the non-Fourier fin problem

Ching-yu Yang *

Department of Mold and Die Engineering, National Kaohsiung University of Applied Sciences, Kaohsiung City 807, Taiwan, ROC

Received 18 June 2004; received in revised form 25 March 2005
Available online 17 May 2005

Abstract

A sequential method is proposed to estimate the periodic boundary conditions on the non-Fourier fin problem. An inverse solution is deduced from a finite difference method, the concept of the future time and a modified Newton–Raphson method. Two examples are used to demonstrate the features of the proposed method. The close agreement between the exact values and the estimated results is made to confirm the validity and accuracy of the proposed method. The results show that the proposed method is an accurate and stable method to determine the periodic boundary conditions in the non-Fourier fin problems.

1. Introduction

During the past decades, several researches have been investigated the fin problems with the periodic thermal loading [1–5]. Most researches solved the problems in Fourier domain [1–4] but only a few solved the problem in non-Fourier domain [5]. Yang [1] derived the analytically solution for a convective fins under a periodic heat transfer. Eslinger and Chung [2] used a finite element method to solve a radiative and convective fin. Aziz and Na [3] adopted a perturbation method to investigate the fins with various thermal properties. Al-Sanea and Mujahid [4] used a finite volume method to study the fins under time-varying boundaries. The above researches are focus on the fin problems with the Fourier effect. However, Lin [5] concluded the non-Fourier effect should be considered in the thermal analysis of a fin when the period of the input temperature frequency is not greater than the thermal relaxation time. Lin's research shows that the thermal waves in the fin system are induced by the delaying response between heat flux and temperature gradient when the periodic thermal conditions are applied. This phenomenon may represent time needed to accumulate energy for signification heat transfer and lead to the thermal wave propagation with a finite speed. Furthermore, there is no work on the inverse non-Fourier fin problems presently. The inverse problem is used to determine the base temperature of the fin from the temperature measured at the fin tip. It is an ill-posed problem because a small measurement error induces a large estimated error [6–14]. Therefore, it is necessary to develop an accurate and stable method to deal with the inverse non-Fourier fin problems with the periodic thermal loading. Through the inverse technique, the unknown periodic boundary conditions at fin base can be deduced indirectly from the temperature measurements at fin tip.

* Tel.: +886 7 381 4526; fax: +886 7 383 5015.
E-mail address: cyyang@cc.kuas.edu.tw

0017-9310/$ - see front matter © 2005 Elsevier Ltd. All rights reserved.
doi:10.1016/j.ijheatmasstransfer.2005.03.018

Nomenclature

A	amplitude of the input temperature
b	thickness of the fin
C	specific heat capacity
$\mathbf{J}$	error function
h_0	heat transfer coefficient, defined as $h_0 = bk/2L^2$
$h(x)$	heat transfer coefficient depend on spatial coordinate
H	dimensionless heat transfer coefficient
k	thermal conductivity
L	length of the fin
N_t	number of the temporal measurements
p	number of grids at spatial coordinate
r	number of the future time
t	temporal coordinate
T	temperature
T_b	periodic boundary condition
T_in	initial temperature of the fin
$\overline{T}_\mathrm{b}$	mean temperature of the periodic boundary condition
T_e	environment temperature
X_m	sensitivity function of θ with respect to the undetermined condition at m-time step
$\mathbf{x}_0$	vector of the initial guess
x	spatial coordinate
Y	measured temperature
ω	dimensionless frequency of the temperature oscillation
$\hat{\omega}$	frequency of the temperature oscillation
ρ	density
τ	relaxation time
$\tau_{i,j}$	error terms of Taylor approximation
β	dimensionless relaxation time
μ	eigenvalue of matrix
η	dimensionless spatial coordinate
ξ	dimensionless temporal coordinate
θ	dimensionless temperature
θ_e	dimensionless environment temperature
θ_m	value of dimensionless temperature at the mth time step
$\mathbf{\Phi}$	vector constructed from Φ
Φ	calculated temperature minus measured temperature
Φ_c	calculated temperature
Φ_meas	measured temperature
$\widehat{\Phi}_u$	component of vector $\mathbf{\Phi}$
ϕ^T_{m+1}	unknown periodic temperature condition at $m+1$th time step
$\mathbf{\Psi}$	sensitivity matrix
$\Psi_{u,v}$	component of vector $\mathbf{\Psi}$
Δ	increment of the search step
ε, δ	value of the stopping criterion
σ	standard deviation of measurement error
λ	intermediate variable
$\lambda_{i,j}$	random number

Subscripts

i, j, m, u, v	indices

Superscripts

exact	exact temperature
meas	measured temperature

Recently, Yang [15] has developed a forward difference method combined with a modified Newton–Raphson method [8] to solve the inverse hyperbolic heat conduction problems. In Yang's research, the coefficients of the governing equation are defined as constants. Then a stable condition for the finite difference implemented in the problem is derived. As well, the modified Newton–Raphson method is used to solve the inverse solution. In this paper, the heat transfer coefficient depends on the spatial coordinate lead to the stable condition for the numerical method is spatial dependent. Therefore, it is need to select the stable condition in the whole spatial domain. Furthermore, the fin problem is under a periodic loading that is more difficult than that of the non-periodic loading.

In this paper, a sequential method combined with the concept of the future time is used to solve the problems step by step. As well, a modified Newton–Raphson method [13,14] is used to search the inverse solution at each time step. In the proposed approach, the determination of the periodic boundary conditions at each time step includes two phases: the process of direct analysis and the process of inverse analysis. In the forward analysis process, the boundary condition is preset and then directed to solve the temperature field of the problem through a finite difference method. Solutions from the above process are substituted into the sensitivity analysis and integrated with the available temperature measured at the sensor's location. Thus, a set of non-linear equation is formulated for the process of the inverse estimation. In the inverse analysis process, the modified Newton–Raphson method is used to guide the exploring points systematically to approach to the undetermined periodic boundary condition. Then, the intermediate boundary is substituted for the unknown boundary in the following analysis. Several iterations are needed for obtaining the undetermined boundary condition. In the present research, the proposed method formulates

the problem from the difference between the calculated temperature and the one measured directly. Therefore, the inverse formulation derived from the proposed method is simpler than that from the non-linear least-squares method.

This paper includes six sections. In the first section, the current researches in the fin problems are introduced and the feature of using the proposed method in the problem is also stated. In the second section, a finite difference formulation for the non-Fourier fin problem is stated and the stable condition for the algorithm is introduced. In the third section, the characteristics of solving the inverse problem are delineated and the content of the concept of the future time, the direct problem, the sensitivity problem, and the algorithm of the proposed method are presented. Meanwhile, the criterion to stop the iterative process is illustrated. In the fourth section, the computational algorithm of the proposed method is shown. Two examples are employed to demonstrate and to discuss the results of the proposed method in the fifth section. In the final section, the overall contribution of this research to the field of inverse heat conduction problem is discussed.

2. Problem statement

The inverse non-Fourier fin problem consists of finding the periodic boundary condition at the fin base while the measured temperature at the fin tip are given. Consider an isolated straight fin with uniform thickness b and length L (see Fig. 1). The ratio $\frac{b}{L}$ is a small value (i.e., $\frac{b}{L} \ll 1$). This fin originally has a uniformly distributed temperature T_{in}. The adiabatic condition is applied to the fin tip $x = L$. At a specific time, a periodic temperature condition $T_{\text{b}} = \overline{T}_{\text{b}} + A\cos(\hat{\omega}t)(\overline{T}_{\text{b}} - T_{\text{in}})$ is applied to $x = 0$ where $\overline{T}_{\text{b}}$ is the mean temperature of the fin base, A is the amplitude of the input temperature and $\hat{\omega}$ is the frequency of the temperature oscillation. On the lateral surfaces, the fin dissipates to environment with a constant temperature T_{e} by convection only. A mathematical formation of the non-Fourier heat conduction is presented as follows:

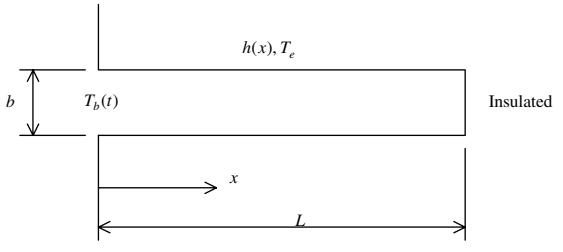

Fig. 1. The fin configuration.

$$k\frac{\partial^2 T(x,t)}{\partial x^2} - 2\frac{h}{b}(T - T_{\text{e}}) = \tau\rho C\frac{\partial^2 T(x,t)}{\partial t^2} + \rho C\frac{\partial T(x,t)}{\partial t} + 2\tau\frac{h}{b}\frac{\partial}{\partial t}(T - T_{\text{e}}) \quad t > 0,\ 0 < x < L \tag{1}$$

$$T(x,0) = T_{\text{in}} \quad 0 \leqslant x \leqslant L \tag{2}$$

$$\frac{\partial T(x,t)}{\partial t} = 0 \quad \text{at } t = 0 \quad \text{and} \quad 0 \leqslant x \leqslant L \tag{3}$$

$$\frac{\partial T(x,t)}{\partial x} = 0 \quad \text{at } x = L \quad \text{and} \quad t > 0 \tag{4}$$

$$T(0,t) = T_{\text{b}} = \overline{T}_{\text{b}} + A\cos(\hat{\omega}t)(\overline{T}_{\text{b}} - T_{\text{in}}) \quad \text{at } x = 0 \quad \text{and} \quad t > 0 \tag{5}$$

where T represent the temperature field $T(x,t)$. k is the thermal conductivity and ρC is the heat capacity per unit volume. τ is the relaxation time that is non-negative. $\overline{T}_{\text{b}}$ is the mean temperature of the fin base, A is the amplitude of the input temperature and $\hat{\omega}$ is the frequency of the temperature oscillation.

The heat transfer coefficient $h(x)$ is dependent on the spatial coordinate and

$$h(x) = h_0 H\left(\frac{x}{L}\right) \tag{6}$$

where h_0 is the heat transfer coefficient that is defined as $h_0 = bk/2L^2$.

The dimensionless governing equation is

$$\beta\frac{\partial^2\theta}{\partial\xi^2} + (1 + \beta H)\frac{\partial\theta}{\partial\xi} = \frac{\partial^2\theta}{\partial\eta^2} - H\theta + H\theta_{\text{e}} \quad \text{at } \xi > 0 \quad \text{and} \quad 0 < \eta < 1 \tag{7}$$

$$\theta(\eta,0) = 0 \quad \text{at } \xi = 0 \quad \text{and} \quad 0 \leqslant \eta \leqslant 1 \tag{8}$$

$$\frac{\partial\theta}{\partial\xi}(\eta,0) = 0 \quad \text{at } \xi = 0 \quad \text{and} \quad 0 \leqslant \eta \leqslant 1 \tag{9}$$

$$\frac{\partial\theta}{\partial\eta}(1,\xi) = 0 \quad \text{at } \xi > 0 \quad \text{and} \quad \eta = 1 \tag{10}$$

$$\theta(0,\xi) = 1 + A\cos(\omega t) \quad \text{at } \xi > 0 \quad \text{and} \quad \eta = 0 \tag{11}$$

where $\eta = \frac{x}{L}, \xi = \frac{\alpha t}{L^2}, \beta = \frac{\alpha\tau}{L^2}, \theta = \frac{T - T_{\text{in}}}{\overline{T}_{\text{b}} - T_{\text{in}}}, \omega = \frac{\hat{\omega}L}{\alpha}$ and $\theta_{\text{e}} = \frac{T_{\text{e}} - T_{\text{in}}}{\overline{T}_{\text{b}} - T_{\text{in}}}$. θ represents the dimensionless temperature field $\theta(\eta, \xi)$. β is the dimensionless relaxation time that is non-negative.

The inverse problem is to estimate the periodic boundary condition $\theta(0,\xi) = 1 + A\cos(\omega t)$ when the temperature field is measured at $\eta = 1$.

3. The direct solution of the hyperbolic equations

The proposed method uses a finite difference method with the equidistant grids along the spatial coordinate and along the temporal coordinate. The finite difference method has been implemented in the researches of Weber [16] and Carey and Tsai [17]. However, the stable

condition of the above researches is not clear. Therefore, the following derivation investigates the stable condition for solving the equation of the non-Fourier fin through an eigenvalue analysis. In this study, the spatial step size is $\Delta\eta$ and the temporal-step size is $\Delta\xi$. The differential terms $\frac{\partial\theta}{\partial\xi}(\eta,\xi)$, $\frac{\partial^2\theta}{\partial\xi^2}(\eta,\xi)$ and $\frac{\partial^2\theta}{\partial\eta^2}(\eta,\xi)$ can be approach by the Taylor series in $\eta=\eta_i$ and $\xi=\xi_j$ as follows:

$$\frac{\partial\theta}{\partial\xi}(\eta_i,\xi_j)=\frac{\theta(\eta_i,\xi_j+\Delta\xi)-\theta(\eta_i,\xi_j)}{\Delta\xi}-\frac{\Delta\xi}{2}\frac{\partial^2\theta}{\partial\xi^2}(\eta_i,\xi_j') \tag{12}$$

$$\frac{\partial^2\theta}{\partial\xi^2}(\eta_i,\xi_j)=\frac{\theta(\eta_i,\xi_j-\Delta\xi)-2\theta(\eta_i,\xi_j)+\theta(\eta_i,\xi_j+\Delta\xi)}{\Delta\xi^2}-\frac{\Delta\xi^2}{12}\frac{\partial 4\theta}{\partial\xi^4}(\eta_i,\xi_j'') \tag{13}$$

$$\frac{\partial^2\theta}{\partial\eta^2}(\eta_i,\xi_j)=\frac{\theta(\eta_i-\Delta\eta,\xi_j)-2\theta(\eta_i,\xi_j)+\theta(\eta_i+\Delta\eta,\xi_j)}{\Delta\eta^2}-\frac{\Delta\eta^2}{12}\frac{\partial^4\theta}{\partial\eta^4}(\eta_i',\xi_j) \tag{14}$$

where $\xi_j'\in(\xi_j,\xi_j+\Delta\xi)$, $\xi_j''\in(\xi_j-\Delta\xi,\xi_j+\Delta\xi)$ and $\eta_i'\in(\eta_i-\Delta\eta,\eta_i+\Delta\eta)$.

Therefore, Eq. (1) can be discretized as the follows:

$$\beta\frac{1}{\Delta\xi^2}[\theta_{i,j-1}-2\theta_{i,j}+\theta_{i,j+1}]+(1+\beta H)\frac{1}{\Delta\xi}[\theta_{i,j+1}-\theta_{i,j}]=\frac{1}{\Delta\eta^2}[\theta_{i-1,j}-2\theta_{i,j}+\theta_{i+1,j}]-H\theta_{i,j}+H\theta_{\mathrm{e}}+\tau_{i,j} \tag{15}$$

where $\tau_{i,j}$ is the error term of Taylor approximation.

After neglect the error term $\tau_{i,j}$ and the difference equation is shown as

$$\left(\frac{\beta}{\Delta\xi^2}+\frac{1+\beta H}{\Delta\xi}\right)\theta_{i,j+1}=\frac{1}{\Delta\eta^2}\theta_{i-1,j}+\left(\frac{2\beta}{\Delta\xi^2}+\frac{1+\beta H}{\Delta\xi}-\frac{2}{\Delta\eta^2}-H\right)\theta_{i,j}+\frac{1}{\Delta\eta x^2}\theta_{i+1,j}+H\theta_{\mathrm{e}}-\frac{\beta}{\Delta\xi^2}\theta_{i,j-1} \tag{16}$$

and

$$\theta_{i,j+1}=\lambda\theta_{i-1,j}+[\lambda(2\alpha\beta+\alpha(1+\beta H)\Delta\xi-H\Delta\eta^2)-2\lambda]\theta_{i,j}+\lambda\theta_{i+1,j}+\lambda\Delta\eta^2H\theta_{\mathrm{e}}-\alpha\beta\lambda\theta_{i,j-1} \tag{17}$$

where $\lambda=\frac{1}{\alpha\beta+\alpha(1+\beta H)\Delta\xi}$ and $\gamma=\lambda(2\alpha\beta+\alpha(1+\beta H)\Delta\xi-H\Delta\eta^2)$.

$$\begin{bmatrix}\theta_{1,j+1}\\ \theta_{2,j+1}\\ \vdots\\ \theta_{p-1,j+1}\end{bmatrix}=\begin{bmatrix}\gamma-2\lambda & \lambda & 0 & \cdots & \cdots & 0\\ \lambda & \gamma-2\lambda & \lambda & \cdots & \cdots & \\ 0 & \cdots & \cdots & \cdots & \cdots & 0\\ \cdots & \cdots & \cdots & \cdots & \cdots & \lambda\\ 0 & \cdots & \cdots & 0 & \lambda & \gamma-2\lambda\end{bmatrix}_{(p-1)\times(p-1)}\times\begin{bmatrix}\theta_{1,j}\\ \theta_{2,j}\\ \vdots\\ \theta_{p-1,j}\end{bmatrix}+\begin{bmatrix}\lambda\theta_{0,j}\\ 0\\ \vdots\\ 0\\ \lambda\theta_{p,j}\end{bmatrix}-\begin{bmatrix}\alpha\beta\lambda & 0 & \cdots & \cdots & 0\\ 0 & \alpha\beta\lambda & \cdots & \cdots & 0\\ \cdots & \cdots & \cdots & \cdots & \cdots\\ \cdots & \cdots & \cdots & \cdots & \cdots\\ 0 & 0 & 0 & \cdots & \alpha\beta\lambda\end{bmatrix}_{(p-1)\times(p-1)}\begin{bmatrix}\theta_{1,j-1}\\ \theta_{2,j-1}\\ \vdots\\ \theta_{p-1,j-1}\end{bmatrix}+\lambda\Delta\eta^2H\theta_{\mathrm{e}} \tag{18}$$

where p is the grid number of spatial coordinate.

The ith eigenvalue of the matrix is determined by the spectral analysis and shows as follows:

$$\mu_i=\gamma-4\lambda\sin\left(\frac{i\pi}{2p}\right)^2 \tag{19}$$

Therefore, the condition for stability is

$$\max\left|\gamma-4\lambda\left(\sin\left(\frac{i\pi}{2p}\right)\right)^2\right|\leqslant 1 \quad \text{where } i=1,2,\ldots,p-1 \tag{20}$$

$$\frac{1}{4}(\gamma-1)\leqslant\lambda\left(\sin\left(\frac{i\pi}{2p}\right)\right)^2\leqslant\frac{1}{4}(\gamma+1) \tag{21}$$

The stability requires that this inequality condition hold as $\Delta\eta\to 0$, i.e., $i=p-1$ and $p\to\infty$

$$\lim_{p\to\infty}\left[\sin^2\left(\frac{p-1}{2p}\pi\right)\right]=1 \tag{22}$$

Therefore, that stability region is confined in

$$\frac{1}{4}(\gamma-1)\leqslant\lambda\leqslant\frac{1}{4}(\gamma+1) \tag{23}$$

where γ and λ are various with the spatial value.

4. The proposed method to estimate the boundary conditions

In each time step, an iterative algorithm is used to estimate the periodic boundary conditions at the fin base while the temperature measured at the fin tip. Some processes are needed in solving the inverse problem. There are the forward problem, the sensitivity problem, the operational algorithm, and the stopping criterion. The forward problem is used to determine the temperature distribution and the sensitivity problem is used to find the search step in the inverse problem. The operational algorithm is used to fulfill the process of the inverse analysis when the solutions of the forward problem

and the sensitivity problem are available. Finally, the stopping criterion is shown to stop the iterative process.

4.1. The forward problem

The proposed method is based on a sequential algorithm and the inverse solution is solved at each time step. Therefore, Eqs. (6)–(10) are limited to only one time step. The transient problem at $t = t_m$ is governed by the following equations:

$$\beta\frac{\partial^2\theta(\eta,\xi_m)}{\partial\xi^2}+(1+\beta H)\frac{\partial\theta(\eta,\xi_m)}{\partial\xi}=\frac{\partial^2\theta(\eta,\xi_m)}{\partial\eta^2}-H\theta(\eta,\xi_m)+H\theta_e \quad \text{at } \xi=\xi_m \quad \text{and} \quad 0<\eta<1 \tag{24}$$

$$\theta(\eta,\xi_{m-1})=\theta_{m-1}(\eta) \quad \text{at } 0\leqslant\eta\leqslant 1 \tag{25}$$

$$\theta(\eta,\xi_m)=\theta_m(\eta) \quad \text{at } 0\leqslant\eta\leqslant 1 \tag{26}$$

$$\frac{\partial\theta}{\partial\eta}(\eta,\xi)=0 \quad \text{at } \xi=\xi_{m+1} \quad \text{and} \quad \eta=1 \tag{27}$$

$$\theta(0,\xi)=\phi^T_{m+1} \quad \text{at } \xi=\xi_{m+1} \quad \text{and} \quad \eta=0 \tag{28}$$

Here, the values of ϕ^T_{m+1} is denoted as the unknown boundary of the periodic temperature.

The inverse solution of the above problem is ill-posed and it is often unstable when the measured data is disturbed by the measurement noise. The concept of future time is used to improve the stability of the estimation in this research. The concept of the future time makes assumptions about the behavior of the experimental data at future time steps, which is included in the measurement to estimate the present state.

When $t = t_m$, the estimated condition between $t = t_{m-1}$ and $t = t_m$ has been evaluated and the problem is to estimate the boundary condition at $t = t_{m+1}$. To stabilize the estimated results in the inverse algorithms, the sequential procedure is assumed temporally that several future values of the estimation are constant [8]. Then, the unknown conditions at the future time are assumed to be constants equal to their present values, i.e.,

$$\phi^T_{m+2}=\cdots=\phi^T_{m+r-2}=\phi^T_{m+r-1}=\phi^T_{m+r}=\phi^T_{m+1} \tag{29}$$

Here r is the number of the future time.

The forward problem, Eqs. (24)–(28), is solved in r steps (from $t = t_{m+1}$ to t_{m+r}) and the undetermined boundaries are set by Eq. (29).

4.2. The sensitivity problem

In the proposed method, the modified Newton–Raphson method is adopted to solve the inverse problem in that the sensitivity analysis is necessary to decide search step. The derivative $\frac{\partial}{\partial\phi^T_{m+1}}$ is taken at both sides of Eqs. (24)–(28). Then, we have

$$\beta\frac{\partial^2 X(\eta,\xi_m)}{\partial\xi^2}+(1+\beta H)\frac{\partial X(\eta,\xi_m)}{\partial\xi}=\frac{\partial^2 X(\eta,\xi_m)}{\partial\eta^2}-HX(\eta,\xi_m) \quad \text{at } \xi=\xi_m \quad \text{and} \quad 0<\eta<1 \tag{30}$$

$$X(\eta,\xi_{m-1})=0 \quad \text{at } 0\leqslant\eta\leqslant 1 \tag{31}$$

$$X(\eta,\xi_m)=0 \quad \text{at } 0\leqslant\eta\leqslant 1 \tag{32}$$

$$\frac{\partial X}{\partial\eta}(\eta,\xi)=0 \quad \text{at } \xi=\xi_{m+1} \quad \text{and} \quad \eta=1 \tag{33}$$

$$X(0,\xi)=1 \quad \text{at } \xi=\xi_{m+1} \quad \text{and} \quad \eta=0 \tag{34}$$

where $X_m=\frac{\partial\theta(\eta,\xi_m)}{\partial\phi^T_{m+1}}$.

Eqs. (29)–(33) describe the mathematical equations for sensitivity coefficient X_m that can be explicitly found. The equation is linear and the dependent variable X_m is with respect to the independent variables η and ξ. Therefore, the sensitive data can be determined directly through a finite difference method.

4.3. A modified Newton–Raphson method

The Newton–Raphson method has been widely adopted to solve a set of non-linear equations. This method is applicable to solve the non-linear problem when the number of the equations and the number of the unknown variables are the same. In the inverse problem, the number of equations is usually larger than the number of variables; therefore a modified version of the Newton–Raphson method is necessary to deal with the inverse problem.

In the present research, the proposed method formulates the problem from the comparison between the calculated temperature and the one measured directly. Therefore, the calculated temperature $\Phi_c(\bar{i},j)$ and the measured temperature $\Phi_{meas}(\bar{i},j)$ at the $\bar{i}$-grid of the spatial coordinate and at j-grid of the temporal coordinate need to be evaluated first. Then, the estimation of the unknown periodic boundary at each time step can be recast as the solution of a set of non-linear equations:

$$\Phi(\bar{i},j)=\Phi_c(\bar{i},j)-\Phi_{meas}(\bar{i},j)=0 \tag{35}$$

where $\bar{i}=0$ and $j = m + 1, m + 2, \ldots, m + r$. r is the number of future time.

The number of equations is the number of the future time r. This detail procedure can be shown as follows:

Substitute the index j from $m + 1$ to $m + r$ and the index $\bar{i}=0$, we have

$$\mathbf{\Phi}=[\Phi(0,m+1),\Phi(0,m+2),\Phi(0,m+3),\ldots,\Phi(0,m+r)]^T=\{\widehat{\Phi}_u\} \tag{36}$$

where $\widehat{\Phi}_u$ is the component of vector $\mathbf{\Phi}$.

The undetermined coefficients are set as follows:

$$\mathbf{x} = \{x_v\} \tag{37}$$

where x_v is the component of vector $\mathbf{x}$.

The derivative of $\widehat{\Phi}_u$ with respect to x_v is solved through Eqs. (30)–(34) and it can be expressed as follows:

$$\Psi_{u,v} = \frac{\partial \widehat{\Phi}_u}{\partial x_v} \tag{38}$$

The sensitivity matrix $\mathbf{\Psi}$ can be defined as follows:

$$\mathbf{\Psi} = \{\Psi_{u,v}\} \tag{39}$$

where $u = 1, 2, 3, \ldots, r$ and $v = 1$ and $\Psi_{u,v}$ is the element of $\mathbf{\Psi}$ at uth row and vth column.

With the starting vector $\mathbf{x}_0$ and the above derivations from Eqs. (36)–(39), we have the following equation:

$$\mathbf{x}_{\lambda+1} = \mathbf{x}_\lambda + \Delta_\lambda \tag{40}$$

Δ_λ is a linear least-squares solution for a set of over-determined linear equations and it can be derived as follows:

$$\mathbf{\Psi}(\mathbf{x}_\lambda)\Delta_\lambda = -\mathbf{\Phi}(\mathbf{x}_\lambda) \tag{41}$$

$$\Delta_\lambda = -[\mathbf{\Psi}^T(\mathbf{x}_\lambda)\mathbf{\Psi}(\mathbf{x}_\lambda)]^{-1}\mathbf{\Psi}^T(\mathbf{x}_\lambda)\mathbf{\Phi}(\mathbf{x}_\lambda) \tag{42}$$

The above derivation is applied at each time step. This method is able to implement in the multi-sensors' measurement. Under this condition, the number of the elements in Eq. (36) is based on the number of measured locations and the number of future times.

4.4. The stopping criteria

The modified Newton–Raphson method (Eqs. (40)–(42)) is used to determine the unknown vector $\mathbf{x}$ defined by Eq. (37). The step size Δ_λ goes from $\mathbf{x}_\lambda$ to $\mathbf{x}_{\lambda+1}$ and it is determined from Eq. (42). Once Δ_λ is calculated, the iterative process to determine $\mathbf{x}_{\lambda+1}$ is executed until the stopping criterion is satisfied.

The discrepancy principle [8] is widely used to evaluate the value of the stopping criterion in the inverse technique. However, the stopping criterion generated from the discrepancy principle does not guarantee the convergence of the inverse solution. Therefore, two criteria are chosen to assure the convergence and to stop the iteration:

$$\|\mathbf{x}_{\lambda+1} - \mathbf{x}_\lambda\| \leqslant \delta\|\mathbf{x}_{\lambda+1}\| \tag{43}$$

$$\|\mathbf{J}(\mathbf{x}_{\lambda+1}) - \mathbf{J}(\mathbf{x}_\lambda)\| \leqslant \varepsilon\|\mathbf{J}(\mathbf{x}_{\lambda+1})\| \tag{44}$$

where

$$\|\mathbf{J}(\mathbf{x}_{\lambda+1})\| = \sum_{i=1}^{p}\sum_{j=1}^{r}[\Phi_c(\bar{i},j) - \Phi_m(\bar{i},j)]^2 \tag{45}$$

where δ and ε are small positive values.

The values of δ and ε are the converge tolerances.

5. Computational algorithm

The procedure for the proposed method can be summarized as follows: First, we choose the number of future times r, the spatial size $\Delta\eta$ of the problem domain, the temporal size $\Delta\xi$, the measured grid and the estimated grid. Given overall convergence tolerance δ and ε and the initial guess $\mathbf{x}_0$. The value of $\mathbf{x}_\lambda$ is known at the λth iteration. Then, the iterative procedure can be summarized as follows:

Step 1. Let $j = m$ and the temperature distribution at $\{\theta_{j-1}\}$ and $\{\theta_j\}$ are known.
Step 2. Collect the measurement $\Phi_{\text{meas}}(\bar{i},j)$ which are $Y^{\bar{i}}_j, Y^{\bar{i}}_{j+1}, \ldots, Y^{\bar{i}}_{j+r-1}$.
Step 3. Assume the initial guess $\mathbf{x}_0$.
Step 4. Solve the forward problem Eqs. (24)–(28), and compute the calculated temperature $\Phi_c(\bar{i},j)$.
Step 5. Integrate the calculated temperature $\Phi_c(\bar{i},j)$ with the measured temperature $\Phi_{\text{meas}}(\bar{i},j)$ to construct $\mathbf{\Phi}$.
Step 6. Calculate the sensitivity matrix $\mathbf{\Psi}$ through Eqs. (30)–(34).
Step 7. Knowing $\mathbf{\Psi}$ and $\mathbf{\Phi}$, compute the step size Δ_λ from Eq. (42).
Step 8. Knowing Δ_λ and $\mathbf{x}_\lambda$, compute $\mathbf{x}_{\lambda+1}$ from Eq. (40).
Step 9. Terminate the process if the stopping criterion (Eqs. (43) and (44)) is satisfied. Otherwise return to step 4.
Step 10. Terminate the process if the final time step is attached. Otherwise, let $j = m + 1$ return to step 2.

6. Results and discussion

In this section, problems defined from Eqs. (1)–(5) are used as examples to estimate the unknown periodic conditions in the fin systems. Two examples are used to demonstrate that the proposed method that can be implemented in the non-Fourier fin heat equations. The discrete sizes of the problem domain are evaluated by Eq. (23) and the proposed finite difference method is used to solve the problem. In example one, the direct solutions of the non-Fourier fin problem are evaluated. In example two, an inverse non-Fourier fin problem with the various input frequency are discussed. The estimated temperature is imposed on the fin base and the temperature is measured at the fin tip. The simulated temperature is generated from the exact temperature in each problem and it is presumed to have measurement error. In other words, the random error of measurement is added to the exact temperature. It can be shown in the following equation:

$$T^{\text{meas}}_{i,j} = T^{\text{exact}}_{i,j} + \lambda_{i,j}\sigma \tag{46}$$

where the subscripts i and j are the grid number of spatial-coordinate and temporal-coordinate, respectively. $T_{i,j}^{\text{exact}}$ in Eq. (46) is the exact temperature. $T_{i,j}^{\text{meas}}$ is the measured temperature. σ is the standard deviation of measurement errors. $\lambda_{i,j}$ is a random number. The value of $\lambda_{i,j}$ is calculated by the IMSL subroutine DRNNOR [18] and chosen over the range $-2.576 < \lambda_{i,j} < 2.576$, which represent the 99% confidence bound for the measured temperature.

Example 1. Consider the problem described in Eqs. (7)–(11) and the parameters defined as $H(\eta) = e^{\eta}$, $A = 0.5$, and $\theta_e = 0.1$.

Fig. 2 shows the temperature distributions for various values β at $\xi = 0.5$. It can be found that the thermal wave travels with a short distance for a larger value of β. This phenomenon is caused by the model induce thermal waves by delaying the response between heat flux and temperature gradient. This delay may represent the time needed to accumulate energy for signification heat transfer and lead to the thermal wave propagation with a finite speed. The sharp discontinuities of this problem can be captured by the proposed method. The oscillation is appeared at discontinuity point of the temperature response and it can be reduced through a smooth process. For illustrate, the oscillation is around $\eta = 0.5$ that is a discontinuity point of the temperature response at $\xi = 0.5$ when $\beta = 1$. When $\beta = 0.1$ and $\xi = 0.5$, the original thermal wave reflected from the direction right to left and then interacted with the new thermal wave from the direction left to right at $\eta = 0.42$. As a result, the result confirmed the validity of the proposed method.

Fig. 3 shows the dimensionless temperature distribution for various values of ω ($\omega = 0.1$, 0.5, 1, and 2) when the relaxation time $\beta = 1$. The results show that the location of the temperature discontinuity is not influenced by the value of ω. Therefore, the speed of the thermal wave propagation is independent on the oscillation frequency of the periodic thermal input.

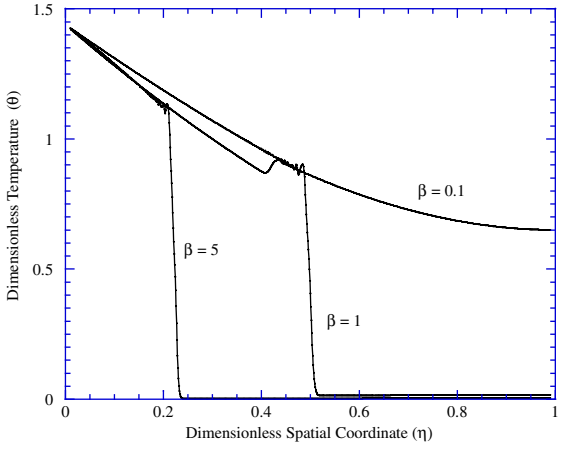

Fig. 2. Temperature distributions for various values of β ($\omega = 1$ and $\xi = 0.5$).

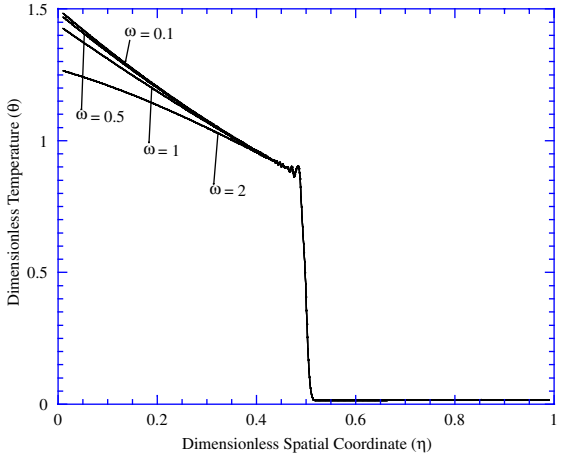

Fig. 3. Temperature distributions for various values of ω ($\beta = 1$ and $\xi = 0.5$).

Example 2. The inverse problem consists of finding the periodic temperature input at the fin base while temperature is measured at the fin tip in Fig. 1. The heat transfer coefficient and the periodic boundary conditions are defined as example one. As well, the relaxation time β is equal to 2.

The periodic input temperature is applied at the side $\eta = 0$ and the temperature measurement at $\eta = 1$. The problems with different frequency ($\omega = 0.1$, 0.5, 1, 2 and 5) are testified in the inverse domain. The spatial domain is divided into 10 intervals and the size of time step is 0.1 that calculated from Eq. (23). One feature of the hyperbolic equation is the heat wave propagates with a finite speed and it is unexpected to estimate the input temperature from the measured temperature immediately. As well, the concept of the future time is adopted to resolve the problem in order to recover the input temperature from the "delay-temperature" measurements.

The numerical results without measurement are shown in Fig. 4 (for $\omega = 0.1$, 0.5, and 1) and Fig. 5 ($\omega = 2$ and 5). In Fig. 4, the numerical results make a good agreement with the exact solution. However, in Fig. 5, the results are deviated from the exact solution due to the coarse sampling time that cannot express the high frequency of the temperature input. Therefore, the discrete sizes at spatial and temporal coordinates need to be refined and they are $\Delta\eta = 0.02$ and $\Delta\xi = 0.02$. The estimated results by the refined grids have a better approximation to the exact ones than that of the previous results (see Fig. 6). Therefore, a fine

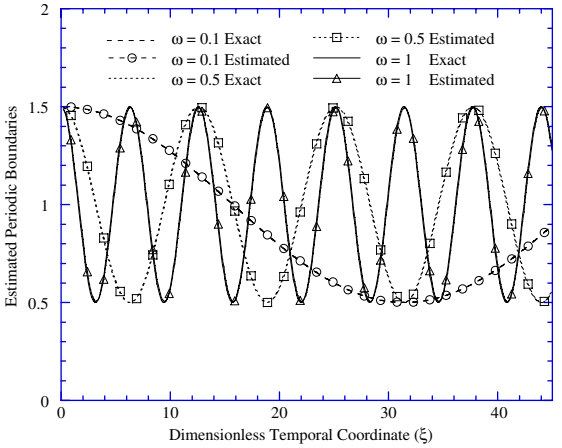

Fig. 4. The estimated results of Example 2 when $\beta = 2$, $r = 14$, $\sigma = 0$, $\Delta\eta = 0.1$, $\Delta\xi = 0.1$, and $\omega = 0.1$, 0.5 and 1.

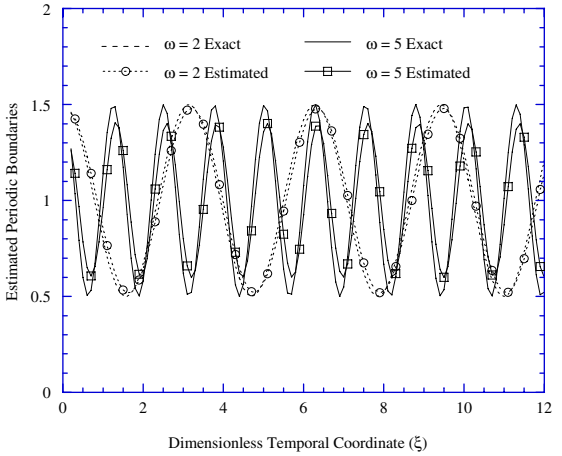

Fig. 5. The estimated results of Example 2 when $\beta = 2$, $r = 14$, $\sigma = 0$, $\Delta\eta = 0.1$, $\Delta\xi = 0.1$, and $\omega = 2$ and 5.

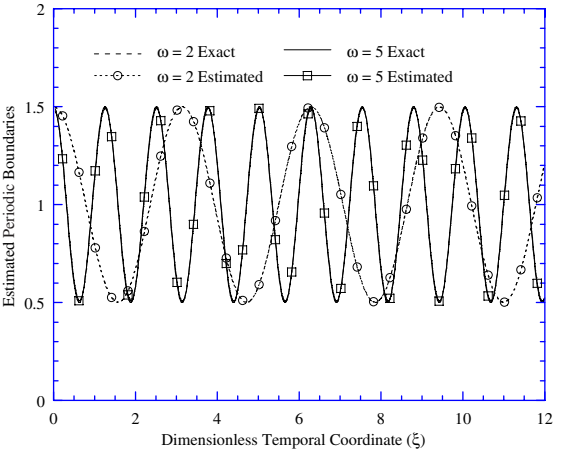

Fig. 6. The estimated results of Example 2 when $\beta = 2$, $r = 72$, $\sigma = 0$, $\Delta\eta = 0.02$, $\Delta\xi = 0.02$, and $\omega = 2$ and 5.

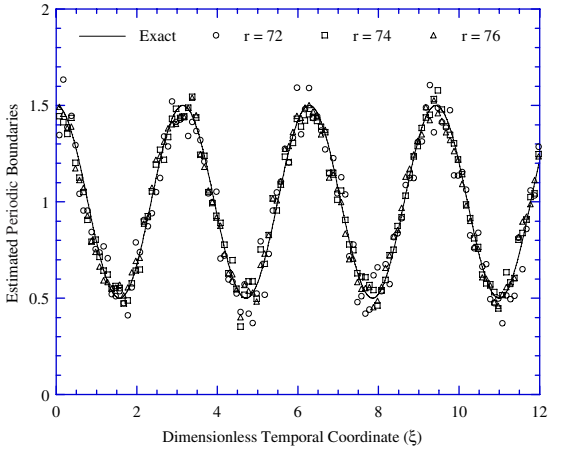

Fig. 7. The estimated results of Example 2 when $\beta = 2$, $\omega = 2$, $\sigma = 0.05$, $\Delta\eta = 0.02$, $\Delta\xi = 0.02$, and $r = 72$, 74, and 76.

mesh is necessary in the periodic temperature input with high frequency.

The inverse solution is also shown in Figs. 7 and 8 when the measurement error is included (i.e., $\sigma = 0.05$ and 0.1). The measurement errors are set within -0.1288 to 0.1288 and within -0.2576 to 0.2576, which implies that the average standard deviation of measurements is 0.05 and 0.1 for a 99% confidence bound, respectively. In Figs. 7 and 8, the accuracy of the estimated results can be improved by the increasing of the future time to seventy-four and seventy-six in this example.

To further investigate the deviation of the estimated results from the exact solution, the relative average errors for the estimated solutions are defined as follows:

$$\mu = \frac{1}{N_t}\sum_{j=1}^{N_t}\left|\frac{f-\hat{f}}{\hat{f}}\right| \tag{47}$$

where f is the estimated result and $\hat{f}$ is the exact result. N_t is the number of the temporal steps. It is clear that a smaller value of μ indicates a better estimation and vice versa.

When measurement errors are not considered, the relative average errors of the estimated results are shown in Table 1. From the results, it shows that the relative errors can be improved through the refined grids for the frequency input. For instance, the case of $\omega = 2$, the value of relative average error is 0.043757 when $\Delta\eta = 0.1$ and $\Delta\xi = 0.1$ and 0.003389 when $\Delta\eta = 0.02$ and $\Delta\xi = 0.02$. When measurement errors are considered, it is seen that the larger measurement error is less

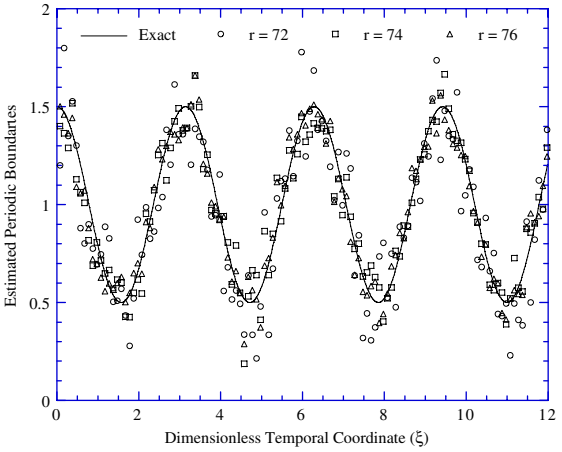

Fig. 8. The estimated results of Example 2 when $\beta = 2$, $\omega = 2$, $\sigma = 0.1$, $\Delta\eta = 0.02$, $\Delta\xi = 0.02$, and $r = 72$, 74, and 76.

Table 1
The relative average errors of example two when $\sigma = 0$

	Relative average error $\Delta\eta = 0.1$, $\Delta\xi = 0.1$ and $r = 14$	Relative average error $\Delta\eta = 0.02$, $\Delta\xi = 0.02$ and $r = 72$
$\omega = 0.1$	0.002285	
$\omega = 0.5$	0.010841	
$\omega = 1$	0.022145	
$\omega = 2$	0.043757	0.003389
$\omega = 5$	0.133720	0.010825
$\omega = 10$	0.294296	0.035067

Table 2
The relative average errors of example two when $\Delta\eta = 0.02$, $\Delta\xi = 0.02$, $\beta = 2$, $\omega = 2$, and $\sigma = 0.05$ and 0.1

	Relative average error $r = 72$	Relative average error $r = 74$	Relative average error $r = 76$	Relative average error $r = 78$
$\sigma = 0.05$	0.087371	0.050208	0.046375	
$\sigma = 0.1$	0.174555	0.098434	0.080672	0.078355

accurate than that of smaller error. For example, when, the value of relative errors is 0.087371 and 0.174555 when $\sigma = 0.05$ and $\sigma = 0.01$, respectively (Table 2).

In this section, the first example demonstrates the validity of the proposed method. In the second example, the proposed method can be implemented in the non-Fourier fin problem with the periodic thermal loading. The numerical result shows that the proposed method is an accurate and robust method to deal with the non-Fourier fin problems when the periodic thermal boundaries are applied.

7. Conclusion

A sequential method has been introduced for determining the periodic thermal conditions in the inverse non-Fourier fin problems. The direct solution at each time step is computed by a finite difference method within a stable interval. As well, the inverse solution at each time step is solved by a modified Newton–Raphson method. The inverse method does not adopt the non-linear least-squares error to formulate the inverse problem, but it is employed a direct comparison of the measured temperature and calculated temperature. Special features about this method are that no preselect functional form for the unknown function is necessary and no non-linear least squares is needed in the algorithm. Two examples have been illustrated based on the proposed method. In the first example, the direct solution of a non-Fourier fin problem is solved. In the second example, the inverse problem of the non-Fourier fin is demonstrated. The results show that the proposed method is able to find both direct and inverse solution of the non-Fourier fin under the periodic thermal conditions. In conclusion, from the results in the examples, it appears that the proposed method is an accurate and stable inverse technique. The proposed method is applicable to other kinds of inverse non-Fourier problems such as source strength estimation in the field of heat conduction problem.

References

[1] Y.W. Yang, Periodic heat transfer in straight fins, J. Heat Transfer 94 (1972) 310–314.
[2] R.G. Eslinger, B.T.F. Chung, Periodic heat transfer in radiating and convecting fins or fin arrays, AIAA J. 17 (1979) 1134–1140.
[3] A. Aziz, T.Y. Na, Periodic heat transfer in fins with variable thermal parameters, Int. J. Heat Mass Transfer 24 (1981) 1397–1404.
[4] S.A. Al-Sanea, A.A. Mujahid, A numerical study of the thermal performance of fins with time-independent boundary, conditions including initial transient effects, Warme Stoffubertrag. 28 (1993) 417–424.
[5] J.Y. Lin, The non-Fourier effect on the fin performance under periodic thermal conditions, Appl. Math. Model. 22 (8) (1998) 629–640.
[6] G. Stolz Jr., Numerical solutions to an inverse problem of heat conduction for simple shapes, ASME J. Heat Transfer 82 (1) (1960) 20–26.
[7] A.N. Tikhonov, V.Y. Arsenin, Solutions of Ill-posed Problems, Winston, Washington, DC, 1977.
[8] J.V. Beck, B.C. Blackwell, R.S. Clair Jr., Inverse Heat Conduction—Ill Posed Problem, Wiley, New York, 1985.

[9] Y. Jarny, M.N. Ozisik, J.P. Bardon, A general optimization method using adjoint equation for solving multidimensional inverse heat conduction, Int. J. Heat Mass Transfer 34 (11) (1991) 2911–2919.
[10] E. Hensel, Inverse Theory and Applications for Engineers, Prentice Hall, Englewood Cliffs, NJ, 1991.
[11] V.A. Morozov, M. Stessin, Regularization Methods for Ill-posed Problems, CRC Press, Inc., Florida, 1993.
[12] O.M. Alifanov, Inverse Heat Transfer Problems, Springer-Verlag, Berlin, Heidelberg, 1994.
[13] C.Y. Yang, Determination of temperature dependent thermophysical properties from temperature responses measured at medium's boundaries, Int. J. Heat Mass Transfer 43 (7) (2000) 1261–1270.
[14] C.Y. Yang, Estimation of boundary conditions in nonlinear inverse heat conduction problems, AIAA J. Thermophys. Heat Transfer 17 (3) (2003) 389–395.
[15] C.Y. Yang, Direct and inverse solutions of the hyperbolic heat conduction problems, AIAA J. Thermophys. Heat Transfer, in press.
[16] C. Weber, Analysis and solution of the ill-posed inverse heat conduction problem, Int. J. Heat Mass Transfer 24 (1981) 1783–1791.
[17] G.F. Carey, M. Tsai, Hyperbolic heat transfer with reflection, Numer. Heat Transfer 5 (1982) 309–327.
[18] User's Manual: Math Library Version 1.0, IMSL Library Edition 10.0, IMSL, Houston, TX, 1987.